THE ASTROPHYSICAL JOURNAL SUPPLEMENT SERIES, 100:413–432, 1995 October

AN *IRAS*-BASED SEARCH FOR NEW DUSTY LATE-TYPE WC WOLF-RAYET STARS

MARTIN COHEN
Radio Astronomy Laboratory, University of California, Berkeley
Received 1994 November 9; accepted 1995 March 23

ABSTRACT

I have examined all *Infrared Astronomical Satellite* (*IRAS*) data relevant to the 173 Galactic Wolf-Rayet (W-R) stars in an updated catalog, including the 13 stars newly discovered by Shara and coworkers. Using the W-R coordinates in these lists, I have examined the *IRAS* Point Source Catalog (PSC), the Faint Source Catalog, and the Faint Source Reject Catalog, and have generated one-dimensional spatial profiles ("ADDSCANs") and two-dimensional full-resolution images ("FRESCOs"). The goal was to assemble the best set of observed *IRAS* color indices for different W-R types, in particular for known dusty late-type WC Wolf-Rayet (WCL) objects. I have also unsuccessfully sought differences in *IRAS* colors and absolute magnitudes between single and binary W-R stars. The color indices for the entire ensemble of W-R stars define zones in the *IRAS* color-color ([12] − [25], [25] − [60])-plane. By searching the PSC for otherwise unassociated sources that satisfy these colors, I have identified potential new W-R candidates, perhaps too faint to have been recognized in previous optical searches. I have extracted these candidates' *IRAS* low-resolution spectrometer (LRS) data and compared the spectra with the highly characteristic LRS shape for known dusty WCL stars. The 13 surviving candidates must now be examined by optical spectroscopy. This work represents a much more rigorous and exhaustive version of the LRS study that identified IRAS 17380 − 3031 (WR98a) as the first new W-R (WC9) star discovered by *IRAS* (Cohen and coworkers). This search should have detected dusty WCL stars to a distance of 7.0 kpc from the Sun, for $|l| > 30°$, and to 2.9 kpc even in the innermost Galaxy. For free-free–dominated W-R stars the corresponding distances are 2.5 and 1.0 kpc, respectively.

Subject headings: circumstellar matter — infrared: stars — stars: Wolf-Rayet — surveys

1. INTRODUCTION

Fewer than 200 Galactic Wolf-Rayet (W-R) stars are currently known (cf. van der Hucht et al. 1988, hereafter HHASD), all but four discovered by optical techniques. Shara et al. (1991, hereafter SPMS) have demonstrated significant incompleteness of the sample of known W-R stars even at distances as close as 2 kpc from the Sun. They estimate that this incompleteness attains 25% for the 2–3 kpc range. Traditional photographic techniques for seeking W-R stars have been superseded by more efficient methods using CCD detectors and narrow passbands designed to isolate specific emission lines or line complexes (e.g., SPMS). Nevertheless, all these techniques are still optically based. While they offer the advantage of reduced confusion in regions of high star density, they are still subject to the vagaries of interstellar extinction. It is, therefore, worthwhile to consider whether the infrared offers a viable alternative in the quest for new W-R stars. While infrared (longward of 2 μm) spectroscopy of W-R stars has been pursued (e.g., Eenens, Williams, & Wade 1991), it has not yet developed into a survey tool to seek new W-R stars. However, the *IRAS* survey affords an extinction of only about 4.5% of A_V at its shortest wavelength (12 μm), and essentially negligible extinction at 25, 60, and 100 μm.

Late-type WC W-R stars (WCLs) frequently have circumstellar dust shells (e.g., Cohen, Barlow, & Kuhi 1975; Gehrz & Hackwell 1974; Williams, van der Hucht, & Thé 1987, hereafter WHT), whose thermal emission dominates both stellar photosphere and free-free emission from stellar winds. This phenomenon becomes more common with lateness of WC subtype. Dust shells can appear as early as type WC4, but only episodically, whereas dust shells are persistent phenomena in the large majority of WC9s studied (WHT). One might well wonder whether dusty WCLs (DWCLs) have been preferentially overlooked or are even invisible in previous optical searches for W-R stars owing to their often substantial circumstellar extinctions (e.g., Cohen & Kuhi (1977a) for Ve 2-45 and GL 2104). Indeed, the most recently discovered WC8–WC10 stars were all recognized in infrared surveys, namely, GL 2104 and GL 2179 (Cohen & Kuhi 1976, 1977b; Allen et al. 1977) from the AFGL Rocket Sky Survey (Price & Walker 1976); WR 48a by Danks et al. (1983); and IRAS 17380−3031 (Cohen et al. 1991). Clearly, a systematic infrared search would provide a valuable adjunct to conventional W-R search techniques.

WCLs (particularly WC9s) show a curious concentration toward the Galactic center (Smith 1968). Newer catalogs of W-R stars (HHASD; Conti & Vacca 1990) have reinforced this early discovery: there is an essentially monotonic trend toward higher Galactocentric radius for the outer edge of the zones containing earlier WC subtypes. Smith & Maeder (1991) explain this confinement of the WCL subtypes to the inner Galaxy in terms of the influence of local initial metallicity (Z) on high-mass stellar evolution: the lower Z, the higher the surface composition ratio of (O + C)/He when the star becomes a WC, hence the earlier the type (at low Z, radiatively driven mass loss is reduced [Abbott 1982; Kudritzki, Pauldrach, & Puls 1987], and newly made C and O are revealed at the surface later in the evolution). Smith & Maeder argue that only in

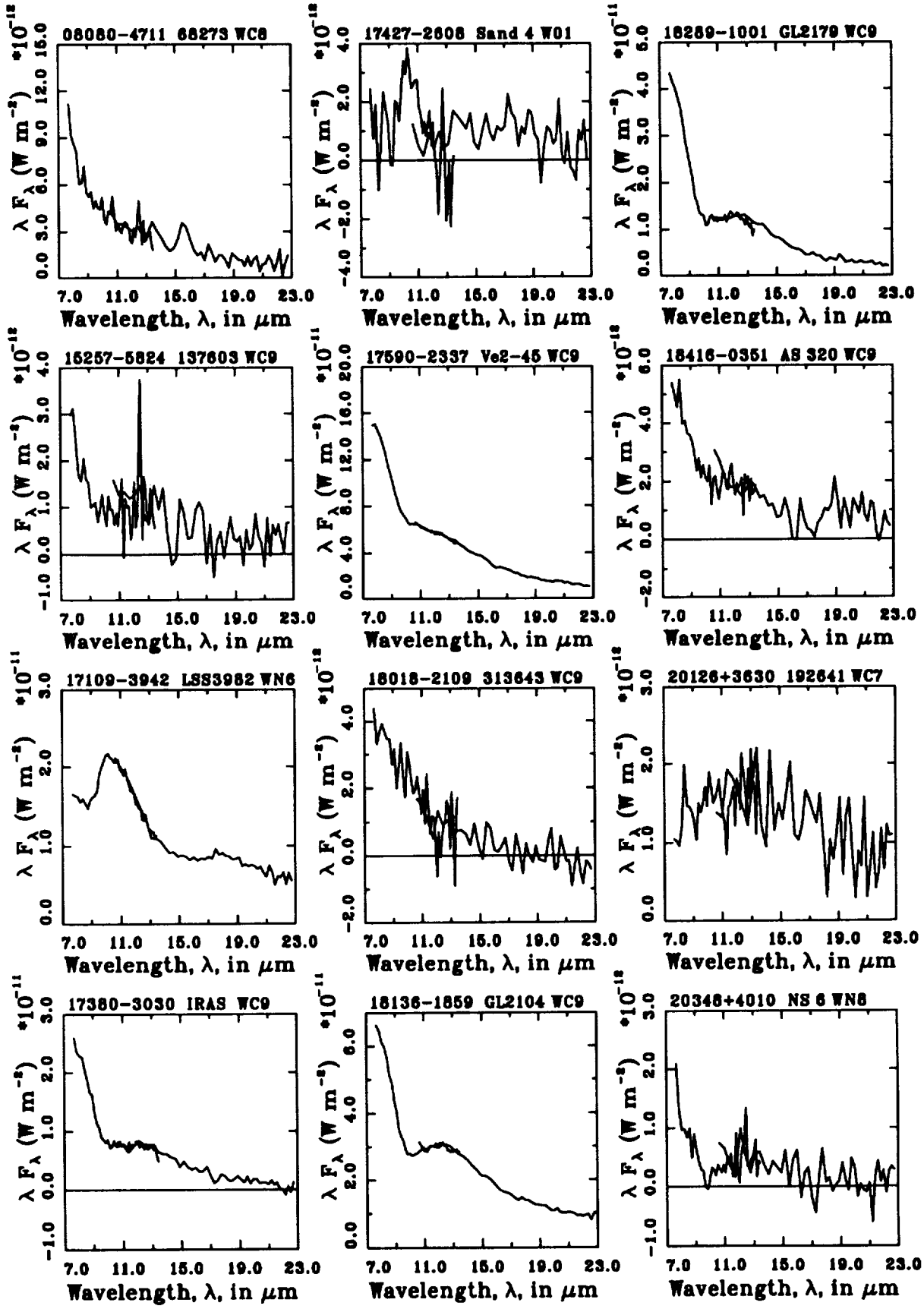

FIG. 1.—Montage of useful LRS spectra for known W-R stars in the form of λF_λ plots

regions of the highest metallicity is it possible to create WCL stars. The combination of new surface abundances with the latest stellar models yields such an elegant explanation for this odd distribution (even given one counterexample) that it merits further study. WC9s, in particular, represent the lowest mass and coolest known W-R stars. It is precisely toward the Galactic center that conventional optical searches for W-R stars would be expected to fail. By contrast, *IRAS* provides an ideal database in which to hunt for W-R stars because of (1) its reduced sensitivity to interstellar extinction close to the Galactic plane, where W-R stars are located; (2) its sensitivity to DWCLs with their infrared-bright dust shells; and (3) its sky coverage (96% complete over the entire sky).

Early photometry of W-R stars from *IRAS* was reported by van der Hucht et al. (1985a), along with spectra from the Dutch low-resolution spectrometer on *IRAS* (Atlas of Low Resolution *IRAS* Spectra 1986, hereafter LRS). The LRS can play a potentially important role in a search for new DWCLs, as discussed below. Indeed, the LRS spectrum of IRAS 17380−3031 was the sole criterion for suggesting that this bright *IRAS* source ($S_{12} \sim 50$ Jy) might be a DWCL (Volk & Cohen 1989), a suggestion only much later vindicated by optical spectroscopy (Cohen et al. 1991).

In the present paper I describe an attempt to find new W-R stars of all types, using an approach based entirely on *IRAS* data but emphasizing DWCLs. Thirteen new DWCL candidates are proposed but must await either optical or near-infrared spectroscopy to test the proposal. Section 2 outlines the role of the LRS; § 3 details the *IRAS* data for W-R stars that were analyzed; § 4 summarizes the *IRAS* color-color analyses of W-R stars; § 5 describes the actual search criteria used to isolate new W-R stars and the candidates identified for future study; § 6 examines the average *IRAS* energy distributions of W-R stars in terms of the emission mechanisms; and § 7 treats the likely completeness of these searches on the basis of the absolute magnitudes for W-R stars dominated by either of the two basic emission processes (dust and free-free).

2. THE ROLE OF THE LRS

Working from coordinates for the established Galactic W-R stars given by HHASD, including the 13 stars found by SPSM and IRAS 17380−3031, I searched the LRS database for positional matches. This LRS survey of all known W-R stars reveals few useful spectra, essentially because W-R stars inhabit the Galactic plane, where *IRAS* suffers the greatest confusion by high source density. The LRS, incidentally, provides a powerful means of rejecting spurious matches, namely, a bright M giant lying within 1′ of the position of WR 85 = LSS 3982, because LRS spectral shapes of different categories of star are already quite well known (cf. Volk & Cohen 1989). The census of 11 relevant and meaningful LRS spectra for known W-R stars is intriguing: one WO1, one WN8, one WC7, one WC8, and seven WC9s. Figure 1 presents these LRS spectra. Even a cursory examination of the DWCL spectra (for AS 320, HDE 313643, GL 2104, IRAS 17380−3031, GL 2179, Ve 2-45, and HD 137603) suggests that these seven WC9s exhibit startlingly similar spectral shapes. This impression is borne out quantitatively by Figure 2*a*, displaying the average of the seven individual LRS spectra (normalized to unity before averaging). The dispersion in shape is quite small and can be enhanced by combining only those spectra with the highest signal-to-noise ratios, namely, those for GL 2104, IRAS 17380−3031, GL 2179, and Ve 2-45 (Fig. 2*b*). The dispersion in shape now has an average of only 3.0%. Using a qualitative version of this technique, Volk & Cohen (1989) argued that IRAS 17380−3031 was a DWCL. Figure 1 shows just how very much like the DWCL IRS spectra known at that time is the LRS spectrum of IRAS 17380−3031. Furthermore, this shape does not typify any other kind of astronomical object, indicating that it might provide a unique criterion for recognizing DWCLs. The shape has been explained by Cohen, Tielens, & Bregman (1989) as a combination of broad 7–9 μm emission by polyaromatic carbon clusters and the effects of interstellar extinction near 10 μm.

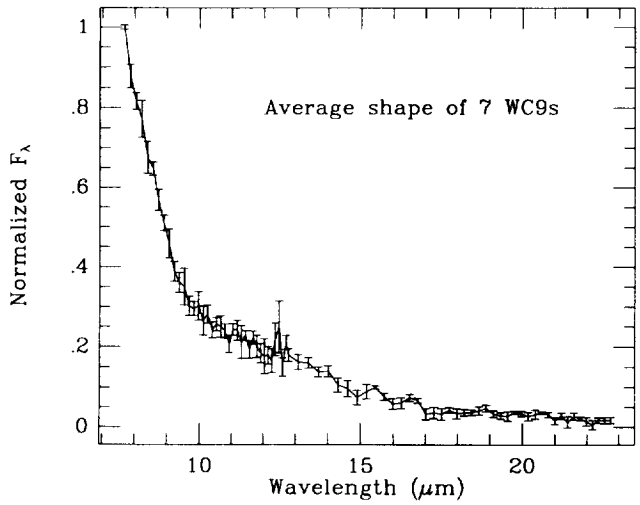

FIG. 2*a*

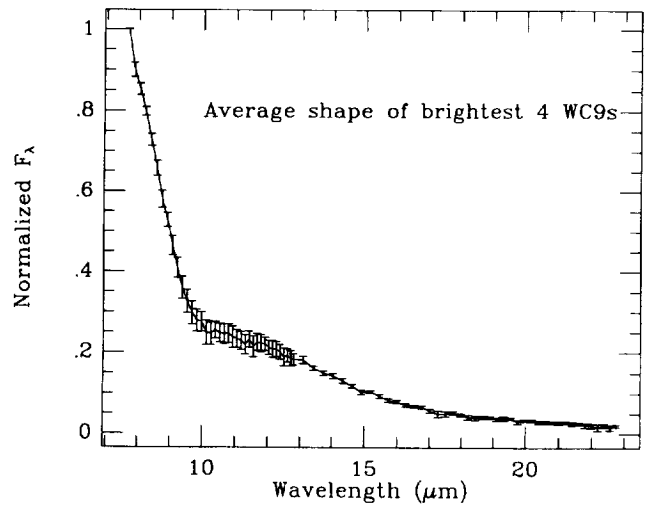

FIG. 2*b*

FIG. 2.—Average of normalized LRS spectra with error bars representing standard errors of the mean. (*a*) For all seven DWCLs. (*b*) For the four DWCLs with highest signal-to-noise ratios in their LRS spectra.

The character of the LRS spectra for the non-WC9 stars shows the following: for HD 68273 (γ^2 Ve [WC8]) a spectrum dominated by free-free emission with a clearly detected [Ne III] emission line (near 15.6 μm: see also Barlow, Roche, & Aitken 1988; van der Hucht & Olnon 1985); for Sanduleak 4 (WO1) the spectrum is equivocal but may also suggest free-free emission from the powerful stellar wind; for HD 192641 (WC7) the spectrum is evidently dominated by thermal emission from circumstellar dust grains; and for NS 6 = AS 431 (WN8) the spectrum appears to show free-free radiation from a stellar wind, with an overlying silicate absorption feature, essentially in accord with the interpretation of the radio and optical spectra (Caillault et al. 1985). Volk et al. (1991, 1992) have extended Volk & Cohen's (1989) flux-limited ($S_{12} \geq 40$ Jy) sample of LRS spectra to *IRAS* thresholds of 20 and 10 Jy. Browsing through the resulting catalogs of spectra for the additional 2652 sources did suggest some possible DWCL-like shapes, but none so convincing in character as that of IRAS 17380−3031. Efforts to enlarge the sample of DWCLs by isolating more *IRAS* sources ostensibly with the "same" characteristic LRS shape have been entirely unsuccessful (M. Cohen 1992, unpublished Anglo-Australian Telescope [AAT] spectroscopy). The likeliest candidate, akin to IRAS 17380−3031, was IRAS 18405−0448, also suggested by Volk & Cohen (1989). But its optical and near-infrared spectra (Williams et al. 1995) indicate an extreme emission-line star, definitely not a WCL star. It seemed obvious that a method for sharpening the *IRAS* source selection criteria was needed, rather than systematic browsing of thousands of LRS spectra to ever-decreasing flux density levels (which alternative, of course, is still being pursued). The LRS could play a valuable role in recognizing new DWCLs if one could sharply restrict the number of *IRAS* sources whose spectra one must examine.

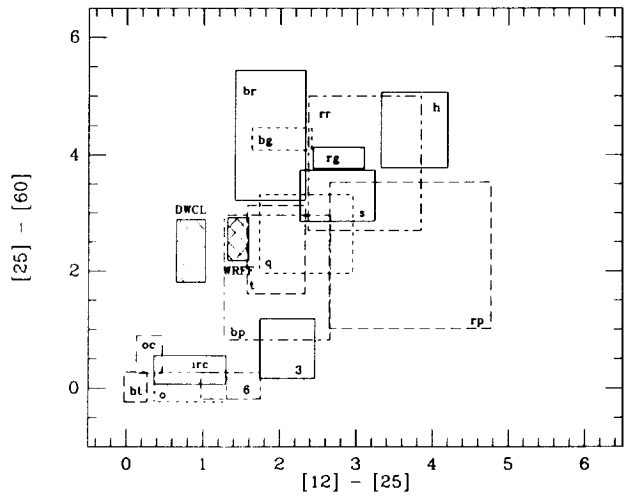

FIG. 3.—"Occupation zones" characterizing different types of source in the *IRAS* [12]—[25]—[60] μm color-color plane. The letter key to different source categories is a more transparent one than that by Walker et al. (1989), but the same zones are represented. *Key*: "bt" = bright normal stars; "o" = O-rich giants; "oc" = optically visible C giants; "irc" = infrared-detectable C giants; "3" and "6" refer to *IRAS* sources with "LRSCHAR" = 3 or 6; "bp" and "rp" = blue and red planetaries; "t" = T Tauri stars; "q" = quasars; "s" = Seyferts; "bg" and "rg" = blue and red galaxies; "br" and "rr" = blue and red reflection nebulae; "h" = H-II regions. The occupation zone corresponding to DWCLs is indicated by the hatched box to the left of the plane; the zone corresponding to all other WRs is the cross-hatched box labeled "WRFF."

3. THE *IRAS*-BASED STRATEGY AND DATA ANALYZED

Walker et al. (1989) have described a practical color-color scheme for separating different categories of astronomical object solely by their *IRAS* attributes. Their "occupation zones" are illustrated by the unhatched boxes in Figure 3 for the *IRAS* [12]—[25]—[60] plane. Each such zone includes 70% of the relevant population of known astronomical sources assembled to define the population's *IRAS* characteristics, so that the zones do overlap, somewhat, outside the box boundaries. However, the hope was that, if one could define a suitably restricted zone corresponding to W-R stars, one might use the *IRAS* broadband colors alone to isolate a sample of sources for subsequent LRS analysis.

The logical route was to assemble every piece of *IRAS* data on all known W-R stars and extract the quintessential attributes for the class. The easiest searches were those through the *IRAS* Point Source Catalog Version 2 (1988, hereafter PSC) and Faint Source Survey databases because relational queries could be run. The PSC and LRS (1986) have existed for many years as relational databases, accessed by INGRES (PSC) or software from SRON, Groningen (LRS), and maintained at the NASA-Ames Research Center. I queried the PSC for all sources within 2′ of the exact coordinates of all the known Galactic W-R stars in an updated catalog provided by van der Hucht (1991). The Faint Source Survey represents the most reliable sources from the entire Faint Source data set (which results from co-adding *IRAS* data from all the separate coverages of the sky), namely, those at preferentially higher Galactic latitudes where confusion is not an issue. At lower latitudes, extracted point sources are passed to the Faint Source Reject Catalog. Both the Faint Source Catalog (FSC) and the Faint Source Reject File (FSRF) (Moshir et al. 1989) exist as relational databases at IPAC, accessed by SYBASE. These were also searched using the same radius as for the PSC. Useful data were found on 64, 1, and 61 W-R stars in the PSC, FSC, and FSRF, respectively.

Because relational searches necessarily involve some limiting radius, there is always the question of whether a "matched" source is truly the W-R star. Therefore, I also examined two-dimensional images that preserved the full spatial resolution of each *IRAS* band, for all W-R stars, at all four wavelengths ("FRESCOs"). Given accurate coordinates, the most reliable way to detect the faintest matches to W-R stars comes from co-adding all the one-dimensional *IRAS* crossings through the W-R star's position ("ADDSCANs"), using two-dimensional images to help disentangle neighboring sources. The several resulting data sets were combined into a unified *IRAS* database for known W-R stars from which *IRAS* attributes could be defined for each of the WN and WC subtypes as well as for the entire class of W-R stars.

Table 1 presents all the data acquired from the *IRAS* catalogs, and indicates the source of each datum ("P" = PSC; "F" = Faint Source Catalog or Reject File; "A" = ADDSCAN; "FR" = FRESCO). In the absence of detections, 3 σ upper limits to flux densities are given. In this context, FRESCO in-

TABLE 1

IRAS PHOTOMETRY FOR GALACTIC WOLF-RAYET STARS
(arranged by HHASD number)

WR	Name(HD)	Spectrum	Data Type	S12 [Jy]	S25 [Jy]	S60 [Jy]	S100 [Jy]
1	4004	WN5	A	0.255	0.12	<0.51	<3.0
			F	0.252	0.184	<0.80	<9.6
			FR	0.217	0.076	<0.62	<3.3
2	6327	WN2	FR	0.069	0.083	<2.4	<8.3
			A	0.033	0.075	0.17	
3	9974	WN3+a(SB1)	A	<0.04	0.038	0.080	<0.29
			FR	0.027	0.032	0.038	<1.4
4	16523	WC5(SB1)	A	0.10	0.065	0.04	<2.4
			FR	0.110	0.059	0.034	<1.2
5	17638	WC6	A	0.16	0.07	<0.40	<5.0
			FR	0.261	0.038	<0.35	<1.5
6	50896	WN5(SB1)	A	1.06	0.58	0.82	<2.7
			P	1.07	0.62	0.81	<4.8
			F	1.00	0.615	0.66:	<1.8
			FR	0.79	0.50	0.62	<4.5
7	56925	WN4	P	<0.29	0.49	9.45	16.9:
			F	<0.14	0.52	<10.	<160.
			A	0.11	0.35		
			FR	<3.3	4.33	cnfsd.	cnfsd.
8	62910	WC4/WN6	A	0.12	0.16	<1.3	<2.5
			F	<0.08	<0.13	0.99	<6.8
			FR	0.126	0.305	cnfsd.	cnfsd.
9	63099	WC5+O7	A	0.155	0.071	0.08	<0.9
			F	0.126	<0.14	<0.7	<6.3
			FR	0.141	0.063	0.34	<4.4
10	65865	WN4.5	FR	0.108	0.064	cnfsd.	cnfsd.
			A	0.110	0.150	0.122	
11	68273	WC8+O9I	A	19.20	8.14	4.36	3.07
			F	20.16	8.71	4.26	<7.5
			P	19.37	8.67	4.26	<13.
			FR	15.53	7.95	3.49	<7.5
12	CD-45 4482	WN7(SB1)	FR	0.085	0.048	cnfsd.	cnfsd.
			A	0.155	0.118		
13	Ve 6-15	WC6	FR	cnfsd.	cnfsd.	cnfsd.	cnfsd.
			A	0.072	0.059		
14	76536	WC6	A	<5.2	<8.7	<2.9	<21.
			FR	cnfsd.	cnfsd.	cnfsd.	cnfsd.
15	79573	WC6	A	0.64	0.31	1.50	
			P	0.56	0.23:	1.76:	<21.
			F	0.64	<0.5	<6.3	<66.
			FR	0.69	0.65	1.68	<42.
16	86161	WN8	P	0.52	0.30	<1.3	<26.
			A	0.48	0.24		
			F	0.45	<0.6	<9.7	<27.
			FR	0.45	0.030	<13.	cnfsd.
17	88500	WC5	FR	0.109	0.027	<0.6	<1.2
			A	0.031	0.060		
18	89358	WN5	FR	<3.2	<7.7	.....	<130.
			A	0.43	0.27		
19	LS 3	WC4	FR	<4.2	<11.	<140.	<280.
			A	0.27	0.34		
19a	SMSP 1	WN7	F	<9.8	<9.3	<160.	<300.
			FR	<40.	<110.	<1200.	<1400.
20	BS 1	WN4.5	FR	<3.1	<3.3	<35.	<78.
			A	0.076	0.079	0.42	1.00
20a	SMSP 2	WN7	FR	cnfsd.	cnfsd.	cnfsd.	cnfsd.
20b	SMSP 3	WN7	FR	cnfsd.	cnfsd.	cnfsd.	cnfsd.
21	90657	WN4+O4-6	P	<0.71	<2.2	<3.4	<26.
			A	0.27			
			FR	<3.8	<2.5	<42.	<66.
22	92740	WN7+a(SB1)	A	1.80	<8.7	cnfsd.	cnfsd.
			F	<22.	<21.	<103.	<770.
			FR	<41.	<162.	cnfsd.	cnfsd.
23	92809	WC6	FR	<28.	<36.	<400.	<1300.
24	93131	WN7+a	FR	<210.	<1800.	<5900.	<4000.
25	93162	WN7+O4f	F	<49.	<360.	<280.	<10500.

TABLE 1—*Continued*

WR	Name(HD)	Spectrum	Data Type	S12 [Jy]	S25 [Jy]	S60 [Jy]	S100 [Jy]
			FR	cnfsd.	cnfsd.	cnfsd.	cnfsd.
26	MS 1	WCE/WN5	FR	<8.3	<4.3	<28.	<88.
27	LS 4	WC6+a	F	<2.9	<3.9.	<560.	<5200.
			FR	<31.	<74.	<730.	<840.
28	MS 2	WN7	A	0.60	1.16		
			FR	cnfsd.	cnfsd.	cnfsd.	cnfsd.
29	MS 3	WN7	FR	<5.5	<6.2	<45.	<130.
30	94305	WC6+O6-8	A	0.07	0.105	0.85:	<5.0
			FR	<2.0	<17.	cnfsd.	cnfsd.
30a	MS 4	WC4+O4	FR	<6.7	<8.6	<68.	<95.
31	94546	WN4+O8V	A	0.135	0.075	<2.1	<16.
			FR	<9.1	<6.4	<53.	<320.
31a	SMSP 4	WC6	P	<0.8	<1.1	<23.	<43.
			A	<0.7	<0.8	<4.6	
			FR	<0.9	<1.8	<150.	<340.
32	MS 5	WC5	FR	<15.	<28.	<130.	<410.
			A	0.145	0.20	1.68	
33	95435	WC5	FR	<0.6	<0.6	<5.7	<14.
			A	0.10	0.060		
34	LS 5	WN4.5	F	<3.0	2.56	<430.	<1400.
			A	0.088	0.19		
			FR	<43.	<87.	<1100.	<1200.
35	MS 6	WN6	FR	<21.	<81.	<320.	<750.
35a	SMSP 5	WN6	FR	<4.5	<12.	<60.	<150.
			A	<1.0	0.12		
35b	SMSP 6	WN4	FR	<7.3	<9.3	<190.	<240.
			A	0.030			
36	LS 6	WN4	FR	<7.2	<7.2	<70.	<115.
			A	0.058	0.15		
37	MS 7	WN3	FR	<7.5	<27.	<240.	<250.
38	MS 8	WC4	FR	<11.	<25.	<320.	<380.
38a	SMSP 7	WN6	FR	<14.	<32.	<290.	<370.
38b	SMSP 8	WC7	FR	<8.2	<28.	<200.	<270.
			A	0.125			
39	MS 9	WC6	FR	<5.9	<20.	<120.	<170.
40	96548	WN8(SB1)	A	0.77	0.30	<0.48	<0.12
			P	0.68	0.25:	<0.58	<10.7
			F	0.69	<0.3	<6.4	<8.5
			FR	0.47	0.29	cnfsd.	cnfsd.
41	LS 7	WC6	FR	<3.5	<4.3	<59.	<130.
			A	0.27			
42	97152	WC7+O7V	FR	<5.0	.....	.....	.....
			A	0.28	0.073		
42a	SMSP 9	WN4.5	FR	<13.	<28.	<320.	<640.
			A	0.10			
42b	SMSP 10	WN3:+C	F	<0.6	<2.2	<56.	<130.
			A	0.131	<1.4		
			FR	<4.9	<29.	<120.	<220.
42c	SMSP 11	WN6	FR	<92.	<270.	<3600.	<5100.
42d	SMSP 12	WN4	FR	<6000.	<39000.	<61000.	<48000.
43	97950	WN6+O5	F	<1100.	<4300.	<5600.	<19000.
			FR	<6300.	<28000.	<27000.	<25000.
44	LSS 2289	WN4	P	<0.8	<0.4	<2.5	<22.
			A	0.023			
			F	<0.8	<0.3	<1.8	<12.
			FR	<23.	<4.1	<8.8	<13.
44a	SMSP 13	WN3:	FR	<56.	<190.	<300.	<530.
			A	0.86	0.38		
45	LSS 2423	WC6	FR	<49.	<220.	<1100.	<1400.
			A	0.31	0.096		
46	104994	WN3p	FR	<34.	<14.	<44.	<85.
47	E311884	WN6+O5V	FR	<1.2	<6.8	<24.	<62.
			A	0.19	0.12		
47a	We 21	WN8	A	0.29	2.15	12.96	<69.
			FR	<7.0	<8.8	<77.	<110.
48	113904	WC6+O9.5I	A	0.50	0.38		

TABLE 1—*Continued*

WR	Name(HD)	Spectrum	Data Type	S12 [Jy]	S25 [Jy]	S60 [Jy]	S100 [Jy]
			P	0.47	<0.2	<1.7	<16.
			F	0.46	<1.0	<0.9	<5.9
			FR	0.25	0.13	cnfsd.	cnfsd.
48a	Danks 1	WC8	FR	<95.	<600.	<1600.	<1700.
49	LSS 2979	WN5	FR	<0.8	<0.9	<7.5	<19.
			A	0.20	0.20		
50	LSS 3013	WC6+a	P	<1.6	1.17	<15.	<88.
			A	0.058	1.05	5.96	
			FR	<1.6	<25.	<160.	<210.
51	LSS 3017	WN4	FR	<8.3	<20.	<260.	<330.
			A	0.24	0.14		
52	115473	WC5	F	0.148	<0.1	<0.8	<11.
			A	0.16	0.18		
			FR	0.058	<0.3	<1.1	<1.7
53	117297	WC8	A	0.59	0.205		
			P	0.68	<1.5	<11.	<98.
			FR	0.179	<4.3	<9.6	<46.
54	LSS 3111	WN4	FR	<2.6	<0.9	<5.5	<12.
55	117688	WN7	P	3.62	2.36	<11.	<71.
			F	3.43	2.60	<56.	<290.
			FR	0.385	<3.1	<18.	<55.
56	LS 8	WC7	FR	<0.96	<3.5	<3.8	<24.
57	119078	WC7	A	0.107	0.155		
			FR	0.060	0.029	<0.77	<1.8
58	LSS 3162	WN4/WCE	FR	<0.4	<0.5	<3.9	<9.4
59	LSS 3164	WC9	FR	<18.	<20.	<190.	<710.
			A	0.60			
60	121194	WC8	FR	<4.3	<6.0	<25.	<150.
			A	0.42	0.19		
61	LSS 3208	WN6	FR	<1.3	<2.4	<4.7	<27.
			A	0.023	0.069		
62	NS 2	WN6	FR	<6.0	<6.2	<32.	<130.
			A	0.30	0.089		
63	LSS 3289	WN6	FR	<23.	<45.	<380.	<860.
			A	0.56	0.36		
64	BS 3	WC7	FR	<1.5	<0.8	<4.3	<22.
			A	0.17	0.049		
65	LSS 3319	WC9	FR	<38.	<33.	<250.	<660.
66	134877	WN8	FR	<6.4	<2.7	<75.	<140.
			A	0.064	0.083	0.29	
67	LSS 3329	WN6	FR	<4.8	<5.7	<49.	.....
			A	0.20			
68	BS 4	WC7	FR	<7.1	<11.	<70.	<160.
			A	0.068	0.113		
69	136488	WC9	A	1.02	0.305	0.71	
			P	0.89	0.20	<0.6	<26.
			F	1.03	0.32	<1.7	<34.
			FR	1.24	0.53	0.52	<11.
70	137603	WC9+B0I	A	6.54	2.09	0.69	<13.
			P	6.53	2.01	<11.	<120.
			F	6.51	2.01	<3.8	<30.
			FR	5.25	1.46	0.99	<14.
71	143414	WN6(SB1)	P	<0.9	<0.2	0.38	3.98:
			A	0.072	0.073		
			F	<0.1	<0.08	0.78	<7.4
			FR	<0.2	<0.2	<2.1	cnfsd.
73	NS 3	WC9	A	0.56	0.23	1.05	3.55
			P	0.50	<0.3	<1.5	<29.
			F	0.54	<0.4	<2.9	<12.
			FR	0.440	0.142	0.826	<9.6
74	BP 1	WN7	A		<107.	<80.	<34.
			P	<155.	<110.	<40.	<390.
			F	<159.	<110.	<84.	<73.
			FR	<160.	<26.	<240.	<260.
75	147419	WN5	FR	<9.8	<24.	<180.	<220.
			A	0.28			

TABLE 1—*Continued*

WR	Name(HD)	Spectrum	Data Type	S12 [Jy]	S25 [Jy]	S60 [Jy]	S100 [Jy]
76	LSS 3693	WC9	P	16.75	34.7:	<2600.	<6800.
			A	16.02	22.83	66.65:	
			FR	<260.	<2200.	cnfsd.	cnfsd.
77	He3-1239	WC8(+a)	P	<2.8	<2.7	<6.0	<150.
			FR	<6.8	<10.	<70.	<150.
78	151932	WN7	A	1.29	0.57		
			P	1.30	0.59	<4.9	<43.
			FR	<1.3	<5.8	<16.	<94.
79	152270	WC7+O5-8	A	0.69	0.415		
			FR	<0.5	<2.7	<14.	<42.
80	LSS 3871	WC9	A	1.88	0.47		
			P	1.88	0.58:	<13.	<130.
			F	1.67	<1.5	<36.	<400.
			FR	1.564	0.280	<65.	<58.
81	He3-1316	WC9	FR	0.462	0.305	<28.	<65.
			A	0.33	0.17		
82	LS 11	WN8	A	0.25	0.23		
			FR	0.156	0.095	<12.	<59.
83	He3-1344	WN6	FR	<2.8	<2.5	<12.	<53.
			A	0.080	0.092	0.15	
84	The 3	WN6	FR	<21.	<26.	<280.	<540.
			A	0.27			
85	LSS 3982	WN6	A	<71.	<52.	<8.4	
			P	<68.	<50.	<6.2	<470.
			F	<62.	<49.	<34.	<91.
			FR	<55.	<38.	<17.	<100.
86	156327	WC7+a	A	0.26	0.215	1.60	
			FR	<1.2	<1.4	<6.2	<31.
87	LSS 4064	WN7	A	0.77	3.72	14.17	
			FR	<2.5	<36.	.....	<20.
88	The 1	WC9	FR	2.58	<47.	<220.	<170.
			A	1.17			
89	LSS 4065	WN7	A	0.39	3.17	21.59	
			P	<3.3	3.49	<50.	<260.
			FR	<2.0	<88.	<200.	<460.
90	156385	WC7	P	0.95	0.47	<0.6	<6.2
			A	0.97	0.28	0.30	
			F	0.81	0.40	<1.0	<8.0
			FR	0.885	0.390	<5.1	<14.
91	StSa 1	WN7	FR	<2500.	<14000.	<44000.	<34000.
92	157451	WC9	A	0.06	0.18	<1.0	
			FR	<0.32	<0.43	<3.5	<5.1
93	157504	WC7+O7-9	FR	<8200.	cnfsd.	cnfsd.	cnfsd.
93a	PKS359+3.1	WN2.5-3	FR	<1.4	<5.0	<1.0	<9.9
			A	0.055	0.10		
94	158860	WN6	FR	<5.7	<6.5	<100.	<190.
			A	0.31			
95	He3-1434	WC9	P	4.56	<1.7	<12.	<200.
			A	4.02	3.39	2.92	
			FR	<41.	<23.	<49.	<120.
96	LSS 4265	WC9	P	1.73	<3.4	<27.	<430.
			A	1.61	0.66		
			F	<1.9	<4.3	<32.	<150.
			FR	0.436	<1.2	<110.	<360.
97	E320102	WN3+O5-7	P	<1.0	<1.9	<1.8	<97.
			A	0.089	0.21	1.38	
			FR	<0.7	<0.8	<9.3	<30.
98	E318016	WC7/WN6	FR	<2.5	<1.6	<44.	<120.
			A	0.54			
98a	IRAS17380	WC9	A	47.84	13.97		
			P	51.63	14.10	<22.	<410.
			F	53.83	13.83	<100.	<1100.
			FR	31.69	11.13	18.91	<810.
100	E318139	WN6	P	4.22	11.08:	95.32	<96.
			A	0.42	0.22	0.39	
			FR	<1.7	<1.3	<6.9	<17.

TABLE 1—*Continued*

WR	Name(HD)	Spectrum	Data Type	S12 [Jy]	S25 [Jy]	S60 [Jy]	S100 [Jy]
101	DA 3	WC8	P	<5.0	<7.0	37.61	<110.
			F	<5.2	<13.	<81.	<340.
			FR	<14.	<38.	<150.	<90.
102	Sand 4	WO1	F	<3.0	8.92	32.56	<4800.
			FR	cnfsd.	cnfsd.	cnfsd.	cnfsd.
103	164270	WC9(SB1?)	A	1.06	0.36	<0.9	
			P	1.03	<1.6	<3.3	<32.
			F	0.88	<0.7	<1.3	<10.
			FR	0.801	0.183	<1.8	<9.0
104	Ve2-45	WC9	A	412.3	133.0	19.94	
			P	411.5	140.2	<38.	<330.
			F	398.8	126.1	<140.	<1300.
			FR	394.21	169.37	<450.	<390.
105	NS 4,Ve2-47	WN8	A	1.80	1.32	<7.1	
			FR	<15.	<27	<140.	<170.
106	E313643	WC9	A	12.04	3.97	14.83	<100.
			P	11.67	3.76	11.69:	<400.
			F	11.20	<8.5	<81.	<440.
			FR	10.22	4.26	20.07	<310.
107	DA 1	WN8	FR	<6.2	<74.	cnfsd.	cnfsd.
			A	2.73			
108	E313846	WN9	FR	<10.	<5.4	<48.	<210.
			A	0.37	0.14		
109	NS 5	WN3	P	<0.2	<0.3	<0.4	<6.6
			FR	<0.5	<0.8	<2.9	<5.1
110	165688	WN6	FR	<17.	<15.	<200.	<650.
			A	0.39	0.47		
111	165763	WC5	A	0.79	0.47	<19.	<37.
			FR	<5.3	<3.6	<17.	<450.
112	GL 2104	WC9	A	159.36	74.59	20.86	<18.
			P	150.4	74.04	19.33	<320.
			F	156.4	72.48	<42.	<180.
			FR	132.76	69.48	12.53	7.33
113	168206	WC8+O8-9IV	P	2.17	2.82:	<120.	<630.
			A	2.63	1.78		
			FR	<18.	<45.	cnfsd.	cnfsd.
114	169010	WC5	P	<500.	<330.	<73.	<260.
			F	<480.	<310.	<63.	<750.
			FR	<34.	<25.	<91.	<120.
115	IC14-19	WN6	A	4.82	4.19	2.81	
			P	<7.7	<4.6	<16.	<250.
			FR	4.35	3.02	<9.8	<16.
116	ST 1	WN8	P	<3.8	8.57	<37.	<190.
			A	0.80	7.97		
			F	<3.1	6.94	<840.	<9400.
			FR	<21.	<75.	<380.	<1000.
117	IC14-22	WC8	P	<2.8	<1.3	<5.1	<54.
			F	<2.8	<1.3	<5.2	<30.
			FR	0.282	0.134	<10.	<16.
118	GL 2179	WC9	A	72.29	21.62	35.29	105.25
			P	70.36	21.69	<37.	<380.
			F	69.82	21.25	<140.	<1000.
			FR	65.15	24.33	31.78	<490.
119	The 2	WC9	FR	1.44	<7.4	<32.	<115.
			A	0.41	0.22		
120	Vy1-3	WN7	FR	<8.8	<11.	<110.	<640.
			A	0.27			
121	AS 320	WC9	A	2.82	1.38	1.77:	
			FR	2.27	1.26	<10.	<260.
123	177230	WN8(SB1)	FR	<0.3	<0.2	<1.5	<3.0
			A	0.090	0.071		
125	IC14-36	WC7	F	0.85	<3.5	<210.	<960.
			A	1.11	1.48		
			FR	<44.	<61.	cnfsd.	cnfsd.
126	ST 2	WC5/WN	P	<0.9	<0.7	<1.4	<7.0
			A	0.065	0.035		

TABLE 1—*Continued*

WR	Name(HD)	Spectrum	Data Type	S12 [Jy]	S25 [Jy]	S60 [Jy]	S100 [Jy]
			F	<0.4	<0.2	<2.6	<13.
			FR	<1.5	<1.8	<4.5	<9.7
127	186943	WN4+O9.5V	FR	<1.2	<3.6	<26.	<27.
			A	0.041			
128	187282	WN4 (SB1)	A	0.040	0.045	0.125	
			FR	0.023	<0.3	<2.9	<3.0
130	LS 16	WN8	P	1.55	13.16	48.22	<50.
			A	1.31	11.70	36.49	29.78
			F	1.66	12.88	38.75	<66.
			FR	1.85	9.44	31.74	47.33
131	IC14-52	WN7+a	P	<0.6	<2.2	<36.	<200.
			F	<1.7	<2.3	<160.	<800.
			FR	<2.9	<7.6	<54.	<100.
132	190002	WC6	P	<0.6	<0.2	<4.8	<54.
			FR	<1.5	<0.6	<3.7	<17.
133	190918	WN4.5+O9.5Ib	A	0.345	0.14	0.42	<6.4
			P	0.34	<0.4	<6.8	<59.
			FR	0.196	0.028	<4.8	<8.8
134	191765	WN6(SB1)	A	0.62	0.39	0.35:	<1.0
			P	0.67	0.31:	<14.	<49.
			FR	0.679	0.378	<6.4	<6.8
135	192103	WC8	A	0.24	0.19	0.31	
			FR	0.141	0.090	<18.	<55.
136	192163	WN6(SB1)	P	1.33	0.58	<6.4	<61.
			A	1.36	0.51		
			F	1.33	<1.3	<19.	<87.
			FR	1.269	0.561	<130.	<51.
137	192641	WC7+OB	A	2.93	2.21	16.60	64.73
			P	3.21	2.37:	26.8:	<200.
			FR	3.564	3.378	<57.	<75.
138	193077	WN6+O9	A	0.36	0.225	0.12	<5.2
			P	0.43	<0.25	<11.	<130.
			FR	0.526	<0.23	<22.	<70.
139	193576	WN5+O6	A	0.59	0.26	0.11	
			P	0.57	<0.48	<18.	<210.
			FR	0.654	0.476	<30.	<39.
140	193793	WC7+04-5	A	1.91	1.04	<1.2	
			P	1.89	1.11	<21.	<210.
			F	1.81	0.94	<12.	<46.
			FR	1.154	0.598	<23.	<110.
141	193928	WN6(SB1)	P	<840.	<240.	<51.	<93.
			FR	cnfsd.	cnfsd.	cnfsd.	cnfsd.
142	ST 3	WO2	FR	<22.	<24.	<51.	<730.
143	195177	WC5	A	0.29	0.32	3.38	<43.
			FR	<5.2	<6.7	<62.	<74.
144	HM19-1	WC4	FR	<7.4	<28.	<260.	<320.
			A	0.37	0.38		
145	AS 422	WN3/WCE(SB1)	P	0.61	<2.7	<42.	<330.
			A	0.55	0.22	0.23:	
			FR	<0.32	<29.	<250.	<220.
146	HM19-3	WC6	P	0.97	<2.2	<20.	<190.
			A	0.84			
			FR	1.218	<17.	<69.	<18.
147	NS 6	WN8	A	5.40	3.03	1.35	
			P	5.30	3.12	<19.	<210.
			F	5.14	<5.9	<7.0	<110.
			FR	3.73:	1.46:	<94.	<130.
148	197406	WN7(SB1)	FR	<0.4	<0.5	<1.8	<4.2
			A	0.11	0.05:		
149	ST 4	WN6-7	FR	<0.8	<0.7	<2.0	<10.
			A	0.080	0.067		
150	ST 5	WC5	A	0.075	0.060	0.30	3.40
			FR	<1.0	<0.9	<4.1	<10.
151	CX Cep	WN4+O8V	FR	<0.8	<1.1	<2.7	<9.6
			A	0.095	0.033		
152	211564	WN3	FR	<2.8	<3.5	<27.	<58.

TABLE 1—*Continued*

WR	Name(HD)	Spectrum	Data Type	S12 [Jy]	S25 [Jy]	S60 [Jy]	S100 [Jy]
153	211853	WN6/WCE+O	FR	<29.	<75.	<440.	<600.
			A	0.25			
154	213049	WC6	FR	<0.5	<0.6	<2.1	<6.8
			A	0.10	0.036		
155	214419	WN7+O	A		0.18	0.09	<0.9
			FR	0.058	0.054	<3.5	<6.9
156	AC+60 38562	WN8	A	0.335	0.27	0.41	0.33
			FR	0.301	0.204	<8.8	<28.
157	219460	WN4.5(+B)	FR	<3.6	<3.3	<49.	<75.
			A	0.17	0.094		
158	AS 513	WN7	A	0.15	0.11	0.125	
			FR	0.308	<2.3	<1.2	cnfsd.

formation was quantitatively valuable in order to evaluate meaningful limits in the absence of detections. In such cases, I evaluated the standard deviation of the emission within an appropriately sized and oriented elliptical aperture at the W-R star's location, and the standard deviation of the sky background emission assessed from between three and 10 locations around the W-R. I then took the root-sum-square (RSS) of the two independent deviations and estimated the upper limit at 3 times this RSS value. A reevaluation of all matches was made in light of clear discrepancies between the different methods of measurement, and particular scrutiny was given to alleged matches with large apparent spatial offsets (greater than 40″–60″).

Notes on two individual stars are in order. I omitted WR 124 because of the intimate association of this WN star with the nebula, M1-67 (Cohen & Barlow 1975; van der Hucht et al. 1985b). AS 320 is the fainter companion of a bright *IRAS* source. Both the PSC and the FSS tabulate the sum of the two objects. ADDSCAN and FRESCO are capable of resolving the objects. Data in Table 1 represent direct measurements of AS 320 with ADDSCAN and FRESCO (the latter at 12 μm only), and independent indirect estimates with FRESCO (subtracting the brighter source's flux densities from the sum of the two sources).

Table 2 represents the weighted combination of all these separate flux estimates, for all the W-R stars, with weights of 3 for F and P, 2 for A, and 1 for FR. If a colon appears after a flux density in Table 1, then weights of 1.5, 1, or 0.5 were used for F or P, A, and FR, respectively. FRESCO's principal value was in deciding how confused a region is, and offering some insight into the P, F, and especially A flux densities, rather than in providing accurate photometry itself. When the background confusion is so high that no meaningful quantitative upper limits can be obtained even with FRESCO, the entry "cnfsd." appears in Tables 1 and 2. In many cases the background may vary so drastically that no useful upper limits can be obtained with an ADDSCAN; in such situations a blank appears in the line. Table 2 is my final *IRAS* archive on the W-R stars themselves, as opposed to their environs.

4. COLOR-COLOR SEPARATIONS

Using standard hot color-corrected *IRAS* magnitudes (e.g., see Wainscoat et al. 1992, § 1), the flux densities were converted into observed magnitudes and hence colors. Before exploring the potential dependence of *IRAS* colors on W-R subclass, we note the unifying approach of Morris et al. (1993), in which it was found that many W-R stars without circumstellar dust emission show a single power-law spectrum from ultraviolet to near-infrared wavelengths, independent of both WN and WC type, and of subclass within these types. These authors felt that these power laws, whose slopes appear to be dependent on mass-loss rate but not on atmospheric abundances, could be extended directly into the mid-infrared on the basis of *IRAS* flux densities reported for three WN stars by Mathis et al. (1992), whose primary interest was in the environs of these W-R stars rather than in the stars themselves. Morris et al. (1993) focused their attention on single W-R stars because of uncertainties in the UV arising from the lack of detailed knowledge of the precise character of the companions. It is, therefore, worthwhile to investigate these authors' hypothesis before proceeding further in the analysis of *IRAS* colors. Specifically, is there *IRAS* evidence for any statistically significant differences between nondusty single and binary W-R stars? (The presence of a hot circumstellar dust shell completely overwhelms any other sources of radiation in W-R stars, whether single or binary.)

Initially, I restrict attention to those W-R stars studied by Morris et al. (1993) and assigned to the "single" or "binary" category by them because information on the power-law spectral character currently exists solely for these stars. Table 3, therefore, summarizes my *IRAS* color data for all nondusty W-R stars, separating these into WN or WC classes and into the single or binary category before recombining them into two samples corresponding to "all-single" and "all-binary" W-R stars. These restricted samples are smaller than the set of W-R stars for which *IRAS* provides useful data; nonetheless, they are meaningful, except for the tiny samples of stars with [60] − [100] colors that I have omitted. I detect no statistically significant ($\geq 3\ \sigma$) differences between single (as defined by Morris et al. 1993) and binary (also so defined) W-R stars in either [12] − [25] or [25] − [60]; i.e., the (mean $\pm$ 3 σ) color ranges of single and binary W-R stars are not distinct. In spite of the absence of any significant distinction, the relevance of binarity is still worth investigating with the larger sample. (One also sees a direct conflict between several stars designated as "single" by Morris et al. yet as "binary" by HHASD, suggesting the merit of a reanalysis.) Table 3, therefore, includes the

TABLE 2

COMBINED *IRAS* PHOTOMETRY FROM ALL DATA SETS

WR	Name(HD)	Spectrum	S12 [Jy]	S25 [Jy]	S60 [Jy]	S100 [Jy]
1	4004	WN5	0.25	0.15	<0.5	<3.0
2	6327	WN2	0.040	0.077	0.17	<8.3
3	9974	WN3+a(SB1)	0.027	0.037	0.072	<0.3
4	16523	WC5 (SB1)	0.10	0.064	0.039	<1.2
5	17638	WC6	0.18	0.064	<0.3	<1.5
6	50896	WN5 (SB1)	1.03	0.60	0.78	<1.8
7	56925	WN4	0.11	0.47	9.45	16.9:
8	62910	WC4/WN6	0.12	0.19	0.99	<2.5
9	63099	WC5+O7	0.14	0.069	0.13	<0.9
10	65865	WN4.5	0.11	0.133	0.12	cnfsd.
11	68273	WC8+O9I	19.38	8.52	4.24	3.07
12	CD-45 4482	WN7 (SB1)	0.14	0.10	cnfsd.	cnfsd.
13	Ve 6-15	WC6	0.072	0.059	cnfsd.	cnfsd.
14	76536	WC6	<5.2	<8.7	<2.9	<21.
15	79573	WC6	0.62	0.34	1.60	<21.
16	86161	WN8	0.48	0.28	<1.3	<26.
17	88500	WC5	0.047	0.053	<0.6	<1.2
18	89358	WN5	0.43	0.27	.....	<130.
19	LS 3	WC4	0.27	0.34	<140.	<280.
19a	SMSP 1	WN7	<9.8	<9.3	<160.	<300.
20	BS 1	WN4.5	0.076	0.079	0.42	1.00
20a	SMSP 2	WN7	cnfsd.	cnfsd.	cnfsd.	cnfsd.
20b	SMSP 3	WN7	cnfsd.	cnfsd.	.....	.....
21	90657	WN4+O4-6	0.27	<2.2	<3.4	<26.
22	92740	WN7+a(SB1)	1.80	<8.7	<100.	<770.
23	92809	WC6	<28.	<36.	<400.	<1300.
24	93131	WN7+a	<210.	<1800.	<5900.	<4000.
25	93162	WN7+O4f	<49.	<360.	<280.	<10500.
26	MS 1	WCE/WN5	<8.3	<4.3	<28.	<88.
27	LS 4	WC6+a	<2.9	<3.9	<560.	<5200.
28	MS 2	WN7	0.60	1.16	cnfsd.	cnfsd.
29	MS 3	WN7	<5.5	<6.2	<45.	<130.
30	94305	WC6+O6-8	0.070	0.10	0.85:	<5.0
30a	MS 4	WC4+O4	<6.7	<8.6	<68.	<95.
31	94546	WN4+O8V	0.14	0.075	<2.1	<16.
31a	SMSP 4	WC6	<0.7	<0.8	<4.7	<43.
32	MS 5	WC5	0.15	0.20	1.68	<410.
33	95435	WC5	0.10	0.060	<5.7	<14.
34	LS 5	WN4.5	0.088	0.19	<430.	<1400.
35	MS 6	WN6	<21.	<81.	<320.	<750.
35a	SMSP 5	WN6	<0.06	0.12	<60.	<150.
35b	SMSP 6	WN4	0.030	<9.3	<190.	<240.
36	LS 6	WN4	0.058	0.15	<70.	<115.
37	MS 7	WN3	<7.5	<27.	<240.	<250.
38	MS 8	WC4	<11.	<25.	<32.	<380.
38a	SMSP 7	WN6	<14.	<32.	<290.	<370.
38b	SMSP 8	WC7	0.13	<28.	<200.	<270.
39	MS 9	WC6	<5.9	<20.	<120.	<170.
40	96548	WN8(SB1)	0.69	0.28	<0.48	<0.12
41	LS 7	WC6	0.27	<4.3	<59.	<130.
42	97152	WC7+O7V	0.28	0.073	.....	.....
42a	SMSP 9	WN4.5	0.10	<28.	<320.	<640.
42b	SMSP 10	WN3:+C	0.13	<2.2	<56.	<130.
42c	SMSP 11	WN6	<92.	<270.	<3600.	<5100.
42d	SMSP 12	WN4	<6000.	<39000.	<61000.	<48000.
43	97950	WN6+O5	<1100.	<4300.	<5600.	<19000.
44	LSS 2289	WN4	0.023	<0.4	<2.5	<22.
44a	SMSP 13	WN3:	0.86	0.38	<300.	<530.
45	LSS 2423	WC6	0.31	0.096	<1100.	<1400.
46	104994	WN3p	<34.	<14	<44.	<85.
47	E311884	WN6+O5V	0.19	0.12	<24.	<62.
47a	We 21	WN8	0.29	2.15	12.96	<69.
48	113904	WC6+O9.5I	0.46	0.33	<0.9	<5.9
48a	Danks 1	WC8	<95.	<600.	<1600.	<1700.
49	LSS 2979	WN5	0.20	0.20	<7.5	<19.
50	LSS 3013	WC6+a	0.058	1.13	5.96	<88.

TABLE 2—*Continued*

WR	Name(HD)	Spectrum	S12 [Jy]	S25 [Jy]	S60 [Jy]	S100 [Jy]
51	LSS 3017	WN4	0.24	0.14	<260.	<330.
52	115473	WC5	0.15	0.18	<0.8	<11.
53	117297	WC8	0.60	0.21	<9.6	<46.
54	LSS 3111	WN4	<2.6	<0.9	<5.5	<12.
55	117688	WN7	0.39	<2.4	<11.	<71.
56	LS 8	WC7	<1.0	<3.5	<3.8	<24.
57	119078	WC7	0.098	0.13	<0.8	<1.8
58	LSS 3162	WN4/WCE	<0.4	<0.5	<3.9	<9.4
59	LSS 3164	WC9	0.60	<20.	<190.	<710.
60	121194	WC8	0.42	0.19	<25.	<150.
61	LSS 3208	WN6	0.023	0.069	<4.7	<27.
62	NS 2	WN6	0.30	0.089	<32.	<130.
63	LSS 3289	WN6	0.56	0.36	<380.	<860.
64	BS 3	WC7	0.17	0.049	<4.3	<22.
65	LSS 3319	WC9	<38.	<33.	<250.	<660.
66	134877	WN8	0.064	0.083	0.29	<140.
67	LSS 3329	WN6	0.20	<5.7	<49.	.....
68	BS 4	WC7	0.068	0.11	<70.	<160.
69	136488	WC9	0.99	0.29	0.67	<11.
70	137603	WC9+B0I	6.53	2.03	0.75	<13.
71	143414	WN6(SB1)	0.072	0.073	0.44	3.98:
73	NS 3	WC9	0.53	0.21	1.01	3.55
74	BP 1	WN7	<107.	<80.	<34.	<73.
75	147419	WN5	0.28	<24.	<180.	<220.
76	LSS 3693	WC9	16.46	26.77	66.65:	<6800.
77	He3-1239	WC8(+a)	<2.8	<2.7	<6.0	<150.
78	151932	WN7	1.30	0.58	<4.9	<43.
79	152270	WC7+O5-8	0.69	0.42	<14.	<42.
80	LSS 3871	WC9	1.79	0.47	<13.	<58.
81	He3-1316	WC9	0.36	0.20	<28.	<65.
82	LS 11	WN8	0.23	0.20	<12.	<59.
83	He3-1344	WN6	0.080	0.092	0.15	<53.
84	The 3	WN6	0.27	<26.	<280.	<540.
85	LSS 3982	WN6	<55.	<38.	<6.2	<91.
86	156327	WC7+a	0.26	0.22	1.60	<31.
87	LSS 4064	WN7	0.77	3.72	14.17	<20.
88	The 1	WC9	1.45	<47.	<220.	<170.
89	LSS 4065	WN7	0.39	3.36	21.59	<260.
90	156385	WC7	0.90	0.40	0.30	<6.2
91	StSa 1	WN7	<2500.	<14000.	<44000.	<34000.
92	157451	WC9	0.06	0.18	<1.0	<5.1
93	157504	WC7+O7-9	<8200.	cnfsd.	cnfsd.	cnfsd.
93a	PKS359+3.1	WN2.5-3	0.055	0.10	<1.0	<9.9
94	158860	WN6	0.31	<6.5	<100.	<190.
95	He3-1434	WC9	4.34	3.39	2.92	<200.
96	LSS 4265	WC9	1.68	0.66	<32.	<150.
97	E320102	WN3+O5-7	0.089	0.21	1.38	<30.
98	E318016	WC7/WN6	0.54	<1.6	<44.	<120.
98a	IRAS17380	WC9	50.34	13.80	18.91	<410.
100	E318139	WN6	0.42	0.22	0.39	<17.
101	DA 3	WC8	<5.0	<7.0	37.61	<110.
102	Sand 4	WO1	<3.0	8.92	32.56	<220.
103	164270	WC9 (SB1?)	0.97	0.33	<0.9	<9.0
104	Ve2-45	WC9	406.19	135.25	19.94	<330.
105	NS 4,Ve2-47	WN8	1.80	1.32	<7.1	<170.
106	E313643	WC9	11.51	3.88	14.68	<100.
107	DA 1	WN8	<6.2	<2.7	cnfsd.	cnfsd.
108	E313846	WN9	0.37	0.14	<48.	<210.
109	NS 5	WN3	<0.2	<0.3	<0.4	<6.6
110	165688	WN6	0.39	<15.	<200.	<650.
111	165763	WC5	0.79	0.47	<17.	<37.
112	GL 2104	WC9	153.59	73.35	19.27	7.33
113	168206	WC8+O8-9IV	2.35	2.13	<120.	<630.
114	169010	WC5	<34.	<25.	<63.	<120.
115	IC14-19	WN6	4.73	3.96	2.81	<16.
116	ST 1	WN8	0.80	7.81	<37.	<190.

TABLE 2—*Continued*

WR	Name(HD)	Spectrum	S12 [Jy]	S25 [Jy]	S60 [Jy]	S100 [Jy]
117	IC14-22	WC8	0.28	0.13	<5.1	<16.
118	GL 2179	WC9	70.32	21.67	34.59	105.25
119	The 2	WC9	0.62	0.22	<32.	<115.
120	Vy1-3	WN7	0.27	<11.	<110.	<640.
121	AS 320	WC9	2.61	1.34	1.77:	<180.
123	177230	WN8 (SB1)	0.090	0.071	<1.5	<3.0
125	IC14-36	WC7	0.95	1.48	<210.	<960.
126	ST 2	WC5/WN	0.065	0.035	<1.4	<7.0
127	186943	WN4+O9.5V	0.041	<3.6	<26.	<27.
128	187282	WN4 (SB1)	0.037	0.045	0.13	<3.0
130	LS 16	WN8	1.55	12.50	41.15	33.29
131	IC14-52	WN7+a	<0.6	<2.2	<36.	<100.
132	190002	WC6	<0.6	<0.2	<3.7	<17.
133	190918	WN4.5+O9.5Ib	0.34	0.12	0.42	<6.4
134	191765	WN6 (SB1)	0.65	0.37	0.35:	<1.0
135	192103	WC8	0.22	0.17	0.31	<55.
136	192163	WN6 (SB1)	1.33	0.55	<6.4	<51.
137	192641	WC7+OB	3.14	2.42	20.00	64.73
138	193077	WN6+O9	0.41	0.23	0.12	<5.2
139	193576	WN5+O6	0.59	0.30	0.11	<39.
140	193793	WC7+O4-5	1.82	1.00	<1.2	<46.
141	193928	WN6(SB1)	<840.	<240.	<51.	<93.
142	ST 3	WO2	<22.	<24.	<51.	<730.
143	195177	WC5	0.29	0.32	3.38	<43.
144	HM19-1	WC4	0.37	0.38	<260.	<320.
145	AS 422	WN3/WCE(SB1)	0.59	0.22	0.23:	<330.
146	HM19-3	WC6	0.95	<2.2	<20.	<190.
147	NS 6	WN8	5.18	3.08	1.35	<110.
148	197406	WN7 (SB1)	0.11	0.05:	<1.8	<4.2
149	ST 4	WN6-7	0.080	0.067	<2.0	<10.
150	ST 5	WC5	0.075	0.060	0.30	3.40
151	CX Cep	WN4+O8V	0.095	0.033	<2.7	<9.6
152	211564	WN3	<2.8	<3.5	<27.	<58.
153	211853	WN6/WCE+O	0.25	<75.	<440.	<600.
154	213049	WC6	0.10	0.036	<2.1	<6.8
155	214419	WN7+O	0.16	0.083	<0.9	<6.9
156	AC+60 38562	WN8	0.33	0.26	0.41	0.33
157	219460	WN4.5(+B)	0.17	0.094	<49.	<75.
158	AS 513	WN7	0.18	0.11	0.13	cnfsd.

TABLE 3

IRAS COLORS OF NONDUSTY SINGLE AND BINARY WOLF-RAYET STARS

Sample	WR type	[12]-[25]	[25]-[60]
Morris et al.	WN - single	1.32±0.18(16)	3.00±0.35(9)
Morris et al.	WN - binary	1.10±0.16(9)	1.98±0.46(5)
Morris et al.	WC - single	1.26±0.19(12)	2.33±0.51(4)
Morris et al.	WC - binary	1.76±0.57(7)	3.71±0.28(5)
Morris et al.	all WRs - single	1.30±0.13(28)	2.80±0.29(13)
Morris et al.	all WRs - binary	1.39±0.27(16)	2.84±0.38(10)
HHASD	WN - single	1.88±0.18(33)	2.92±0.28(15)
HHASD	WN - binary	1.11±0.12(21)	2.56±0.31(11)
HHASD	WC - single	1.22±0.14(22)	3.40±0.44(6)
HHASD	WC - binary	1.52±0.41(10)	3.29±0.48(6)
HHASD	all WRs - single	1.62±0.13(55)	3.04±0.24(21)
HHASD	all WRs - binary	1.24±0.16(31)	2.82±0.27(17)

TABLE 4

IRAS COLORS OF DIFFERENT TYPES OF WOLF-RAYET STARS

WR type	[12]–[25]	[25]–[60]	[60]–[100]
WN2	2.30 (1)	2.81 (1)	(0)
WN2.5	2.26 (1)	(0)	(0)
WN3	1.72±0.54(4)	2.89±0.59(3)	(0)
WN4	1.67±0.43(6)	4.14±1.07(2)	1.94 (1)
WN4.5	1.45±0.34(5)	2.99±0.58(3)	2.25 (1)
WN5	1.12±0.13(5)	1.52±0.72(2)	(0)
WN6	1.24±0.18(12)	2.28±0.39(6)	3.71 (1)
WN7	1.78±0.44(8)	3.16±0.56(3)	(0)
WN8	1.96±0.39(11)	2.80±0.49(5)	1.08±0.01(2)
WN9	0.54 (1)	(0)	(0)
All WNs	1.56±0.12(54)	2.76±0.21(25)	2.01±0.48(5)
WO1	(0)	3.36 (1)	(0)
WO2	(0)	(0)	(0)
WC4	1.85±0.13(3)	3.75 (1)	(0)
WC5	1.33±0.13(10)	3.31±0.57(5)	3.95 (1)
WC6	1.46±0.18(8)	3.88±0.18(3)	(0)
WC7	1.19±0.22(10)	3.34±0.85(3)	2.59 (1)
WC8	0.91±0.17(6)	1.90±0.70(2)	0.96 (1)
WC9	0.76±0.17(17)	2.08±0.36(11)	1.82±0.78(3)
All WCs	1.12±0.11(54)	2.79±0.26(25)	2.16±0.54(6)
All WRs	1.34±0.09(108)	2.78±0.16(51)	2.09±0.35(11)
All free-free WRs	1.46±0.10(87)	2.58±0.28(39)	2.14±0.47(7)
Non-dusty WCs	1.31±0.15(33)	3.19±0.32(13)	2.45±1.49(2)
All DWCLs	0.84±0.13(21)	2.35±0.39(12)	2.01±0.58(4)

same analysis of *IRAS* colors, but now based on HHASD's designations of single and binary for the entire sample of W-R stars in Table 2. I dropped the hybrid stars from consideration in this context because of their potentially ambiguous interpretation as single or composite stars, but assigned to the binaries any W-R star with a type of "SB1" or "SB2" (spectroscopic binaries), or "+O" (companion assigned a spectral type, usually O type), or "+a" (absorption lines detected in the spectrum). Although single WN stars tend to be redder in the mean than binaries, neither WC stars alone nor the sample of all W-R stars can sustain any statistically significant distinction between the (mean ± 3 σ) color ranges of single and binary systems.

Consequently, Table 4 summarizes the separate average [12] − [25] colors for W-R stars of all subtypes, distinguishing WNs from WCs. The colors [25] − [60] and [60] − [100] are essentially all the same for WN and WC types and show no trends. Hybrid stars were assigned to the category corresponding to their dominant subtype (that given first). The average for all WNs is [12] − [25] = 1.56 ± 0.12 (54 stars), [25] − [60] = 2.76 ± 0.21 (25 stars); for all WCs it is 1.12 ± 0.11 (54 stars) and 2.79 ± 0.26 (25 stars), respectively.

These colors indicate a definite "blueward" trend with lateness of subtype for [12] − [25] among the WC stars, whereas WNs show no pattern (Fig. 4). To sharpen the search for DWCLs, I also tabulate the colors for known DWCLs based on the set of 25 WCs established to show either permanent or variable dust emission (see Williams & van der Hucht 1992). I have *IRAS* data for 21 of these stars that define a DWCL color zone centered on [12] − [25] = 0.84 ± 0.13, [25] − [60] = 2.35 ± 0.39, [60] − [100] = 2.01 ± 0.58. The average for all WN, WO, and WC stars is [12] − [25] = 1.34 ± 0.09 (108 stars) and [25] − [60] = 2.78 ± 0.16 (51 stars).

By removing all these DWCLs, one can define the colors of nondusty WCLs too (Table 4). The WNs, early-type WCs (WCEs), and nondusty WCLs show no statistically significant color differences, suggesting that all these stars are dominated by a common emission mechanism at least from 12 to 100 μm.

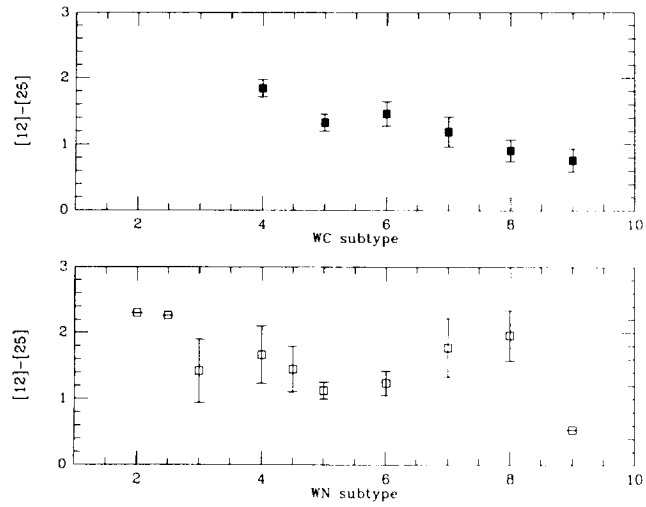

FIG. 4.—Mean *IRAS* [12] − [25] colors of W-R stars, distinguishing WC and WN types (see Table 4).

Consequently, I have also created colors for the ensemble of "all others," meaning all W-R stars excluding only DWCLs (the two WO stars are included here too). Thus there are two separate color-color zones to represent DWCLs and all other W-R stars. The hatched rectangle in Figure 3 corresponds to the 12—25—60 μm zone characteristic for DWCLs (with extent in each axis of ± 1.39 σ about the mean color). The cross-hatched rectangle in Figure 3 likewise represents all nondusty W-R stars. (Note that Fig. 3 is not identical to the Walker et al. 1989 diagram. They used non–color-corrected colors, whereas I have presented Fig. 3 in the same context as the W-R colors, namely, with hot color correction: the differences in occupation zone boundaries amount to only 0.03 mag in [12] − [25] and 0.07 mag in [25] − [60].)

Morris et al. (1993) found the mean spectral index characterizing the short-wavelength power laws of W-R stars to be −2.85 [in $F_\lambda(\lambda)$ terms], corresponding to a color index, [12] − [25], of 0.95. None of the mean color indices in Table 3 is as small as this value, although there are certainly some individual stars with colors near 0.95 and even lower values too. Morris et al. demonstrated that their power-law spectra appear to continue to 25 μm for the three WN stars studied using *IRAS* data by Mathis et al. (1992), namely, W-R 6, W-R 40, and W-R 136. These *IRAS* spectral indices were estimated as −2.7, −3.2, and −3.0. My own values of [12] − [25] imply spectral indices for these stars of −2.7, −3.2, −3.2, in close agreement with Mathis et al. However, most W-R stars show slopes closer to −2.0 between 12 and 25 μm, such as optically thin free-free emission from their stellar winds would produce. They are close to a slope of −2.8 between 25 and 60 μm on the basis of their mean color indices, probably indicative of increasing optical depth at longer wavelengths. Morris et al. (1993) concluded that there must be a substantial contribution from free-free emission to the short-wavelength continua of W-R stars. It would take a detailed side-by-side investigation of W-R stars to establish whether exactly the same power-law continuum found for W-R stars between the ultraviolet and the near-infrared extends into the *IRAS* wavelength region. For the present we note simply that all nondusty W-R stars appear to be consistent with a continuum, largely due to free-free emission, that stretches from the ultraviolet into the *IRAS* wavelength range.

One can understand the differences in color and even intuit approximately where the W-R populations should lie. Monochromatic flux densities for zero magnitude, ZMF_λ, are defined by the photospheric spectrum of a hot star such as Sirius, falling roughly as λ^{-4}. Thus, the ratio $(ZMF_{12}/ZMF_{25}) \sim 18.8$. Assuming (1) that all nondusty single W-R stars are characterized by simple power laws, as Morris et al. have established, at least for single stars, (2) that the *IRAS* measurements of binary W-R stars are negligibly contaminated by photospheric radiation from any secondary, and (3) that the typical slope of these power laws is dictated by optically thin free-free emission which has $F_\lambda \propto \lambda^{-2}$, one would expect a free-free flux density ratio, F_{12}/F_{25}, of ~4.3. Therefore, the free-free color index is expected to be

$$[12] - [25] = -2.5 \log[(F_{12}/F_{25})/(ZMF_{25}/ZMF_{12})], \quad \text{or} \sim 1.6.$$

Similarly, W-R stars dominated by thermal emission from hot dust have not attained their Rayleigh-Jeans domain, so $F_\lambda \propto \lambda^{-3}$, hence the flux density ratio F_{12}/F_{25} should be ~9.0, leading to a dust color index of [12] − [25] ~ 0.8. From Tables 3 and 4 one finds that the free-free dominated W-R stars have about 1.5 as their mean value of [12] − [25], while the DWCLs (Table 4) have [12] − [25] of about 0.8, both similar to these rough estimates, reinforcing this interpretation of the *IRAS* energy distributions of nondusty and dusty W-R stars. (The actual mean value of [12] − [25] observed for all nondusty W-R stars, namely, 1.46, corresponds to a power law with slope −2.2, still quite close to optically thin free-free.)

5. THE SEARCH FOR NEW WOLF-RAYET CANDIDATES

5.1. *DWCLs*

Note (Fig. 3) that DWCLs are essentially distinct from all other types of source, while the main body of W-R stars—those emitting predominantly free-free radiation; see below—overlaps considerably the zone for "blue planetary nebulae," and to a lesser extent that for "T Tauri stars" (see also Walker et al. 1989, their Table 1). This relative isolation suggests the potential value of a color-color search of the PSC. The specific "core query" made to identify new DWCL candidates was $0.649 \leq [12] - [25] \leq 1.024$, $1.809 \leq [25] - [60] \leq 2.885$, $|b| < 5°$, with no associations to catalogs other than *IRAS*, and having FQUAL = 333*. Very few W-R stars are detected at 100 μm, and there is always danger of cirrus contamination, so I chose not to use the additional [60] − [100] color constraint, to avoid possible rejection of otherwise viable W-R candidates. (In fact, virtually all those candidates that passed the LRS shape criterion were undetected at 100 μm and would, indeed, have been lost at this stage, had the third color been required.)

The definition of an occupation zone implies that only ~70% of any normally distributed population lies in the 2.78 σ wide box. I would like to be more complete for the DWCLs; therefore, I doubled the color zone searched to $0.461 \leq [12] - [25] \leq 1.211$, $1.271 \leq [25] - [60] \leq 3.423$, corresponding to over 99% of a normally distributed population. There is, of course, no guarantee that the rather limited number of W-R stars in the Galaxy are normal in their color distributions, so this more conservative approach seems justified. I also included as candidates any PSC source whose mean *IRAS* colors lay outside this broader search area but whose colors overlapped the query box at the mean ± 1 σ level, using the actual uncertainties in the source colors, as constructed from the relevant pairs of PSC "RELUNCs."

The broader INGRES query on the PSC using these criteria yielded 219 candidates. I extracted all LRS spectra for each of these candidates, finding spectra to exist for 132 sources (a total of over 500 individual spectra, typically four per candidate). Many objects are, of course, very faint to *IRAS*, and their LRS spectra are correspondingly noisy. However, a total of 13 *IRAS* sources (in both hemispheres) was returned, having LRS spectral signatures quantitatively like those of the known DWCLs. Their locations in the sky need to be examined for optical counterparts, then pursued spectroscopically (or at least using pairs of narrow passbands isolating WC line and continuum regions in a CCD survey). A viable alternative may be near-infrared low-resolution spectroscopy (near 2 μm)

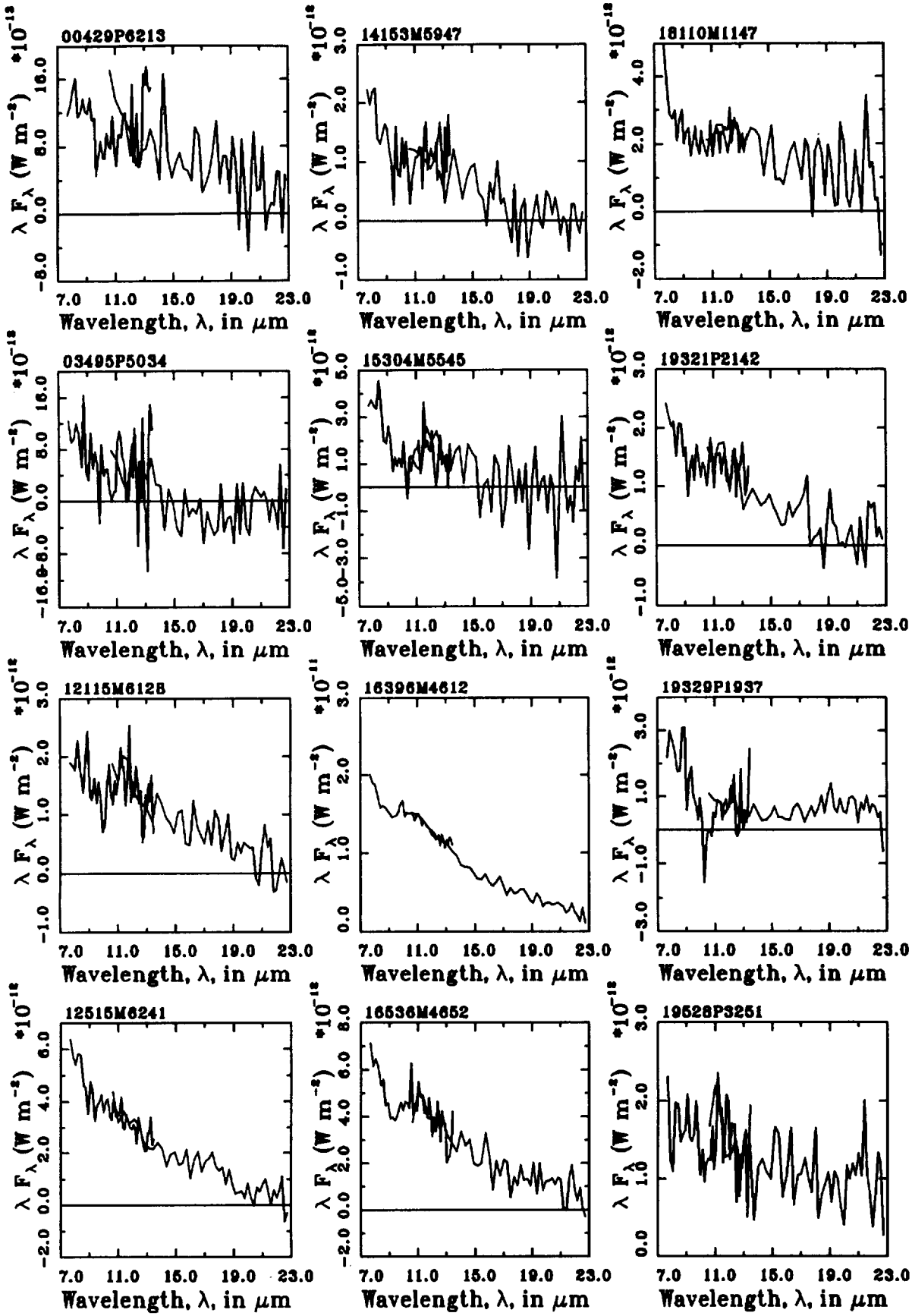

FIG. 5.—LRS spectra of the 13 DWCL candidates

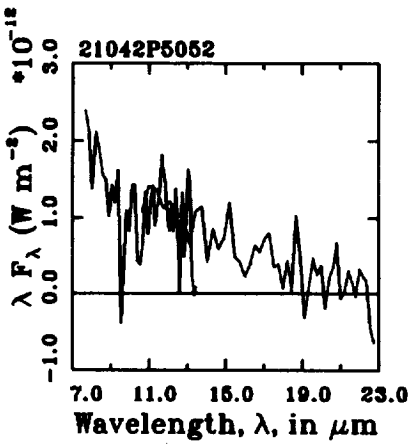

FIG. 5—*Continued*

that is readily capable of detecting the broad bright emission lines of W-R stars (cf. Eenens et al. 1991). Table 5 gives the *IRAS* names and 1950 coordinates of these 13 sources, four of which (those with asterisks in the table) were returned by the core query [$\pm 1.39\ \sigma$] and the remaining nine by the broader search [$\pm 2.78\ \sigma$]). Figure 5 plots their *IRAS* LRS spectra (compare with Fig. 2).

5.2. *Other Wolf-Rayet Stars*

Identically constructed queries on the PSC, with core and doubly broadened searches using the occupation zone for all other (free-free–emitting) W-R stars (Table 4), resulted in 70 sources being returned, of which 28 have an LRS spectrum. Only one of these, however, looked quantitatively like a free-free spectrum, namely, that for IRAS 19537+2608. Figure 6 presents this LRS spectrum, and its coordinates are appended to Table 5. This single source emerged from the core query, $1.318 \leq [12] - [25] \leq 1.588$, $2.182 \leq [25] - [60] \leq 2.918$; no other additional free-free–dominated W-R candidates were found in the broader search.

TABLE 5

NAMES AND COORDINATES OF *IRAS* DWCL AND FREE-FREE EMISSION CANDIDATES[a]

IRASNAME	RA(1950)	DEC(1950)
DWCLs		
00428+6213	$00^h42^m53.6^s$	+62°13′33″
03495+5034	03 49 31.6	+50 34 16
12114–6128*	12 11 30.0	–61 28 31
12515–6241	12 51 32.8	–62 41 54
14153–5947*	14 15 22.7	–59 47 32
15304–5545*	15 30 24.4	–55 45 18
16396–4613	16 39 39.4	–46 13 07
16538–4652	16 53 51.4	–46 52 40
18110–1148	18 11 01.9	–11 48 13
19321+2141	19 32 11.1	+21 41 54
19329+1937*	19 32 58.5	+19 37 25
19528+3251	19 52 49.5	+32 51 38
21041+5052	21 04 11.5	+50 52 32
Free-free WRs		
19537+2608*	19 53 43.9	+26 08 41

[a] *IRAS*NAMEs with asterisks indicate sources returned by the "core" queries; others come from the broader searches.

6. NATURE OF THE ENERGY DISTRIBUTIONS OF WOLF-RAYET STARS

It is instructive to examine the mean colors for DWCLs and all nondusty W-R stars in terms of their implied *IRAS* energy distributions. To do this, one normalizes each energy distribution at 12 μm and calculates the successive F_λ values via the magnitudes at 25, 60, and 100 μm derived from the color indices. The DWCL spectrum can be broken into a 500 K blackbody that fits the entire flux at 12 and 25 μm, and about 17% of that at 60 μm, and a 38 K blackbody to account for the remaining 60 μm and all the 100 μm fluxes. The rough characteristic scale of the 500 K dust envelope is about 3600 R_* from the WC star's surface. Assuming that the long-wavelength component is not simply cirrus contamination then, if the cold dust were also heated by direct but diluted starlight, it would lie at about $2.8 \times 10^5\ R_*$. This component could represent either interstellar material swept up by the W-R stellar wind or conceivably the remnant of an ancient episode of dust formation.

Analysis of a similarly constructed average energy distribution for all nondusty W-R stars indicates that, if one attributes the 12 and 25 μm fluxes entirely to optically thin free-free emission, there is still significant long-wavelength radiation that is not accounted for (if one uses a steeper power law such as Morris et al. 1993 find typical of W-R stars at shorter wavelengths, there is already an excess at 25 μm, hence my use of the flatter optically thin spectrum). This has a color temperature of ~45 K and might again be dusty interstellar material swept up by the powerful stellar winds, whether or not it is associated with a visible nebula or "bubble" (as are many W-R stars).

7. COMPLETENESS OF THE SEARCH FOR NEW WOLF-RAYET STARS

By using distances from Conti & Vacca (1990) (who used a homogeneous set of intrinsic colors to determine W-R dis-

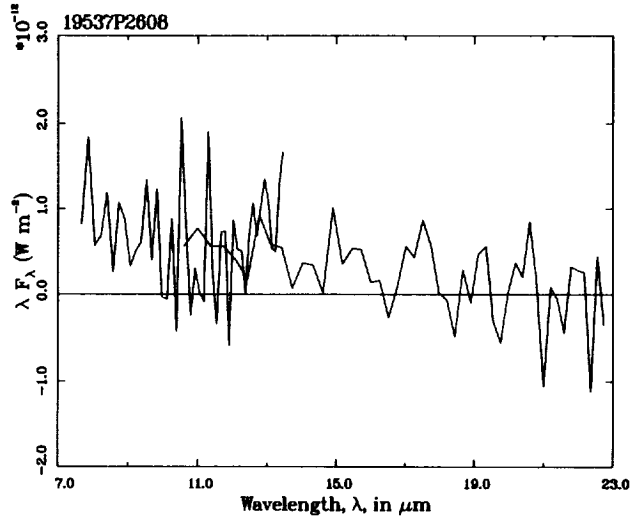

FIG. 6.—LRS spectrum of the single free-free–dominated W-R candidate.

TABLE 6

ABSOLUTE *IRAS* MAGNITUDES OF NONDUSTY SINGLE AND BINARY WOLF-RAYET STARS

WR sample	M_{12}	M_{25}	M_{60}
WN - single	-7.21±0.17(39)	-9.08±0.26(32)	-12.18±0.45(14)
WN - binary	-6.75±0.22(23)	-7.74±0.26(20)	-10.15±0.63(10)
WC - single	-6.96±0.26(23)	-7.93±0.21(19)	-10.71±0.53(5)
WC - binary	-6.01±0.22(11)	-7.55±0.50(10)	-11.06±0.94(7)
All WRs - single	-7.12±0.14(62)	-8.65±0.20(51)	-11.80±0.38(19)
All WRs - binary	-6.51±0.17(34)	-7.68±0.24(30)	-10.52±0.53(17)

tances via reddening), in conjunction with Table 2, absolute *IRAS* magnitudes of W-R stars were also defined, to assess the volume likely to have been sampled by *IRAS*. I excluded Conti & Vacca's (1990) distances of 34 kpc for WR 64 = BS 3, and 27 kpc for WR 49 = LSS 2979, preferring to believe that these two stars either have nonstandard optical colors or dubious photometry. (At these distances, these two stars were outstandingly brighter than all other W-R stars.) The issue of whether there is any distinction between single and binary W-R stars is again worth investigating, in terms of its potential effects on their absolute magnitudes. The magnitudes are summarized in Table 6 on the basis solely of the larger single and binary samples definable from Table 2 using HHASD's spectral types to determine binarity. The single W-R stars seem to be systematically more luminous than the binaries, perhaps suggesting that secondaries interfere with, or even truncate, the W-R stellar winds. However, this effect is not statistically significant: the $\pm 2\ \sigma$ bands around the mean colors of single and binary W-R stars are overlapping. Therefore, I have recombined the single and binary W-R stars and have broken them down again into WN and WC subtypes (Table 7). The absolute magnitudes for the set of all WNs are not statistically distinct from those of nondusty WCs, so I further combined the two types into the set of all W-R stars dominated by free-free emission.

To calculate the distances to which an *IRAS* PSC survey for W-R stars is complete, consider the following. Cohen's (1994) latest version of the SKY model for the point-source sky replicates the pattern of *IRAS* source counts across the entire sky quite well. By comparing the apparent magnitudes at which the observed *IRAS* (cumulative) counts depart from SKY's predicted counts, one gains an estimate of the true limits for the onset of *IRAS* incompleteness as a function of Galactic direction. There are essentially two distinct regimes. In the inner Galaxy, $|l| \leq 30°$, $|b| \leq 2°$, source surface densities on the sky are so high that *IRAS* is complete only to $[12] \approx +3.4$ and $[25] \approx +1.8$. Once the latitude exceeds $\sim 2°$ from the plane or

TABLE 7

ABSOLUTE *IRAS* MAGNITUDES OF DIFFERENT TYPES OF WOLF-RAYET STARS

WR type	M_{12}	M_{25}	M_{60}	M_{100}
WN2	-6.13 (1)	-8.43 (1)	-11.25 (1)	(0)
WN3	-5.88±1.08(5)	-7.28±1.24(4)	-11.63±0.31(2)	(0)
WN4	-6.31±0.25(10)	-8.28±0.36(6)	-12.85±2.06(2)	-16.85 (1)
WN4.5	-6.73±0.45(6)	-7.89±0.75(5)	-10.54±1.01(3)	-14.67 (1)
WN5	-6.21±0.32(5)	-7.36±0.33(4)	-9.13±0.11(2)	(0)
WN6	-7.55±0.21(17)	-9.00±0.34(13)	-11.61±0.63(6)	-17.53 (1)
WN7	-7.40±0.33(11)	-8.93±0.54(8)	-12.36±1.09(3)	(0)
WN8	-7.43±0.26(10)	-9.21±0.52(10)	-12.21±1.15(4)	-14.28±2.42(2)
WN9	-6.96 (1)	7.50 (1)	(0)	(0)
All WNs	-6.99±0.15(66)	-8.58±0.21(52)	-11.33±0.42(24)	-15.52±0.89(5)
WC4	-6.44±0.18(2)	-8.40±0.06(2)	-12.09 (1)	(0)
WC5	-6.63±0.56(10)	-7.46±0.34(9)	-10.07±0.80(4)	-15.89 (1)
WC6	-6.66±0.42(9)	-7.84±0.58(8)	-13.07±1.01(3)	(0)
WC7	-6.47±0.23(11)	-7.65±0.32(9)	-11.32±1.45(3)	-16.37 (1)
WC8	-7.72±0.37(6)	-8.62±0.42(6)	-12.27±2.76(3)	-9.42 (1)
WC9	-10.03±0.51(19)	-10.97±0.55(17)	-13.96±0.76(11)	-16.50±1.62(3)
All WCs	-7.85±0.30(57)	-8.89±0.31(51)	-12.64±0.56(25)	-15.20±1.36(6)
All DWCLs	-9.67±0.52(21)	-10.51±0.50(21)	-13.95±0.69(11)	-16.47±1.15(4)
All non-dusty WCs	-6.78±0.22(36)	-7.77±0.21(30)	-10.61±1.06(14)	-12.66±3.23(2)
All WRs	-7.39±0.16(123)	-8.74±0.18(103)	-12.00±0.36(49)	-15.35±0.81(11)
All free-free WRs	-6.91±0.12(102)	-8.28±0.16(82)	-11.07±0.47(38)	-14.70±1.13(7)

the longitude is well within the 30°–220° range, then source confusion is far less of a problem, and incompleteness is typically not encountered until [12] $\approx$ +5.3 and [25] $\approx$ +3.7. To calculate the incompleteness limits for this *IRAS*-based search, one need only establish the maximum volume in which [12] − [25] and [25] − [60] are available for an *IRAS* source within the PSC. At 60 μm the density of extended sources (typically H II regions) dictates the degree of confusion in the inner Galaxy. However, the great sensitivity of *IRAS* at this long wavelength, coupled with the intrinsically high W-R luminosities, suggests that the requirement that [25] − [60] be available does not reduce the survey depth determined from the requirement that [12] − [25] exists.

From the absolute magnitudes in Table 7, one therefore concludes that, in the high source density regime, [12] − [25] is complete to 1.0 kpc for free-free–emitting W-R stars and to 2.9 kpc for DWCLs. Outside $|l| < 30°$, however, the search is complete to 2.9 and 7.0 kpc, for free-free–emitting and dusty W-R stars, respectively. These distances are 1.28 and 3.08 kpc for innermost and outer Galactic regimes if one simply treats all W-R stars as a single class. All of these volumes greatly exceed those associated with optical searches for W-R stars, as anticipated.

8. CONCLUSIONS

There is a weak tendency for single W-R stars to be more luminous at *IRAS* wavelengths than binaries, possibly indicative of a truncation of the W-R star's stellar wind by its companion. However, the *IRAS* attributes (absolute magnitudes and colors) of single and binary nondusty W-R stars are not statistically distinct. I conclude that it is possible to characterize the *IRAS* colors of both DWCLs and free-free–dominated W-R stars sufficiently sharply that *IRAS* color-based searches for new W-R candidates of both types are possible. Whether I have been successful can be determined only through follow-up observations. Either way, this infrared search is complete in a volume much larger than that accessible to optical techniques. Note that Table 5 does suggest potential DWCLs that are not toward the Galactic center. Should any of these stars in the outer Galaxy be shown truly to be a WC9 star, then the tantalizing idea of Smith & Maeder (1991), that metallicity governs the Galactic distribution of the WCLs, will have been disproved

This effort was partially supported by NASA under grant NAG 5-2015 with the University of California, Berkeley. I also thank NASA-Ames for partial support under cooperative agreement NCC 2-142 with UC Berkeley. I acknowledge the valuable assistance at IPAC of Debbie Levine, Ann Wehrle, and Sue Terebey in using the SYBASE query language, in obtaining and assembling the many ADDSCANs and FRESCO images, and in using SKYVIEW to process the latter. I am also grateful to Peter Conti for his thorough review of the paper and for making several valuable suggestions.

REFERENCES

Abbott, D. C. 1982, ApJ, 259, 282
Allen, D. A., Hyland, A. R., Longmore, A. J., Caswell, J. L., Goss, W. M., & Haynes, R. F. 1977, ApJ, 217, 108
Atlas of Low Resolution *IRAS* Spectra. 1986, *IRAS* Science Team, prepared by F. M. Olnon & E. Raimond, A&AS, 65, 607 (LRS)
Barlow, M. J., Roche, P. F., & Aitken, D. K. 1988, MNRAS, 232, 821
Caillault, J.-P., Chanan, G. A., Helfand, D. J., Palterson, J., Nourek, J. A., Takalo, L. O., Bothun, A. D., & Becker, R. H. 1985, Nature, 313, 376
Cohen, M. 1994, AJ, 107, 582
Cohen, M., & Barlow, M. J. 1975, Astrophys. Lett., 16, 165
Cohen, M., Barlow, M. J., & Kuhi, L. V. 1975, A&A, 40, 291
Cohen, M., & Kuhi, L. V. 1976, PASP, 88, 535
———. 1977a, MNRAS, 180, 37
———. 1977b, PASP, 89, 829
Cohen, M., Tielens, A. G. G. M., & Bregman, J. D. 1989, ApJ, 344, L13
Cohen, M., van der Hucht, K. A., Williams, P. M., & Thé, P. S. 1991, ApJ, 378, 302
Conti, P. S., & Vacca, W. D. 1990, AJ, 100, 431
Danks, A. C., Dennefeld, M., Wamsteker, W., & Shaver, P. A. 1983, A&A, 118, 301
Eenens, P. R. J., Williams, P. M., & Wade, R. 1991, MNRAS, 252, 300
Gehrz, R. D., & Hackwell, J. A. 1974, ApJ, 194, 619
IRAS Point Source Catalog Version 2, Vols. 2–6. 1988, Joint *IRAS* Science Working Group (NASA RP-1190; Washington, DC: GPO) (PSC)
Kudritzki, R. P., Pauldrach, A., & Puls, J. 1987, A&A, 173, 293
Mathis, J. S., Cassinelli, J. P., van der Hucht, K. A., Prusti, T., Wesselius, P. R., & Williams, P. M. 1992, ApJ, 384, 197
Morris, P. W., Brownsberger, K. R., Conti, P. S., Massey, P., & Vacca, W. D. 1993, ApJ, 412, 374
Moshir, M., et al. 1992, Explanatory Supplement to the *IRAS* Faint Source Survey (Pasadena: JPL)
Price, S. D., & Walker, R. G. 1976, The AFGL Four Color Infrared Sky Survey (AFGL TR-76-0208)
Shara, M. M., Potter, M., Moffat, A. F. J., & Smith, L. F. 1991, in IAU Symp. 143, WR Stars and Interrelations with Other Massive Stars in Galaxies, ed. K. van der Hucht & B. Hidayat (Dordrecht: Kluwer), 591 (SPMS)
Smith, L. F. 1968, MNRAS, 141, 317
Smith, L. F., & Maeder, A. 1991, A&A, 241, 77
van der Hucht, K. A. 1991, private communication
van der Hucht, K. A., Hidayat, B., Admiranto, A. G., Supelli, K. R., & Doom, C. 1988, A&A, 199, 217 (HHASD)
van der Hucht, K. A., Jurriens, T. A., Olnon, F. M., Thé, P. S., Wesselius, P. R., & Williams, P. M. 1985a, A&A, 145, L13
———. 1985b, in Birth and Evolution of Massive Stars and Stellar Groups, ed. W. Boland & H. van Woerden (Dordrecht: Reidel), 167
van der Hucht, K. A., & Olnon, F. M. 1985, A&A, 149, L17
Volk, K., & Cohen, M. 1989, AJ, 98, 931
Volk, K., Kwok, S., Stencel, R. S., & Brugel, E. W. 1991, ApJS, 77, 607
Volk, K., Stencel, R. S., Brugel, E. W., & Kwok, S. 1992, private communication
Wainscoat, R. J., Cohen, M., Volk, K., Walker, H. J., & Schwartz, D. E. 1992, ApJS, 83, 111
Walker, H. J., Cohen, M., Volk, K., Wainscoat, R. J., & Schwartz, D. E. 1989, AJ, 98, 2163
Williams, P. M., Cohen, M., van der Hucht, K., Bouchet, P., & Vacca, W. D. 1995, MNRAS, in press
Williams, P. M., & van der Hucht, K. 1992, in ASP Conf. Proc. 22, Non-isotropic and Variable Outflows from Stars, ed. L. Drissen, C. Leitherer, & A. Nota (San Francisco: ASP), 269
Williams, P. M., van der Hucht, K. A., & Thé, P. S. 1987, A&A, 182, 91 (WHT)